International Journal of Thermal Sciences 48 (2009) 2171–2178

Contents lists available at ScienceDirect

International Journal of Thermal Sciences

journal homepage: www.elsevier.com/locate/ijts

Validity of pseudo-gas-side-controlled models to predict the behaviour of desiccant matrices

C.R. Ruivo*, J.J. Costa, A.R. Figueiredo

ADAI, Departamento de Engenharia Mecânica, Universidade de Coimbra, 3030-788 Coimbra, Portugal

ARTICLE INFO

Article history:
Received 11 January 2008
Received in revised form
8 April 2009
Accepted 8 April 2009
Available online 17 May 2009

Keywords:
Adsorption
Desiccant layer
Transfer coefficients
Pseudo-gas-side-controlled model

ABSTRACT

In the present work, a detailed model of simultaneous heat and mass transfer through a desiccant microporous media of an element of a channel wall of compact desiccant matrix was used to numerically evaluate the overall transfer coefficients of pseudo-gas-side-controlled models (PGSCMs). In the detailed modelling, the relevant phenomena considered within the porous medium are the surface diffusion of adsorbed water, Knudsen diffusion of water vapour, heat conduction and the sorption process. The convective mass and heat fluxes predicted by the detailed model are used to estimate the evolution of the pseudo-global resistances to heat and mass transfer during a sorption process, which are required by the PGSCM. The simplified formulation of the PGSCM is presented for an element of the channel wall of the desiccant matrix.

Results of the evolutions of these pseudo-global resistances are presented for a wide range of values of the layer thickness of the porous medium, which is supposed to be silica gel RD. It is concluded that the pseudo-gas-side-controlled model with constant transfer coefficients is valid only for layer thicknesses lower than 0.1 mm, approximately.

1. Introduction

A significant number of studies were carried out to predict the behaviour of solid desiccant air dehumidification systems using simplified mathematical models [1–11]. In most of them, the heat and mass transport phenomena occurring inside the porous desiccant medium are not described in a very detailed way, simplified approaches being adopted instead.

Numerous studies have been devoted to the modelling of desiccant wheels, but further research is still needed [12], namely to analyse the influence of the variation of the properties, either of the moist air and of the desiccant materials, which are taken as constant in most of the models. It is also recognized that the accuracy of many of the existing models must be improved taking into account the internal diffusion phenomena.

Pseudo-gas-side-controlled models (PGSCMs) have been used in some works [5], which require overall heat and mass transfer coefficients to account for the internal resistances in the desiccant layer. A single-blow test procedure for compact heat and mass transfer exchangers to evaluate those overall transfer coefficients is presented in [13]. The pseudo-gas-side-controlled model can be seen as a modified gas-side-controlled model (GSCM), the main difficulty laying on the estimation of the pseudo-mass transfer coefficients to be used in a particular simulation. The range of validity of such models can be investigated by using experimental techniques or by detailed numerical modelling.

When advanced numerical methods are used to solve the complete set of differential transport equations, a number of critical issues still remain, such as the lack of suitable functions to describe the variation of the porous medium properties [14–17] and the complexity of numerically solving the intrinsically coupled phenomena within the porous desiccant solid, together with the great computational time needed [7]. Nevertheless, advanced mathematical models for sorption and transport phenomena – including surface diffusion of the adsorbed phase, Knudsen diffusion of the gaseous phase and thermal diffusion – as local processes in the porous desiccant layer have been adopted to support numerical predictions of the behaviour of desiccant and enthalpy wheels [17–23].

Some studies focused on the detailed modelling of the behaviour of a wall channel element of a hygroscopic matrix have been conducted with the main purpose of investigating the validity of

* Corresponding author. Área Departamental de Engenharia Mecânica, Instituto Superior de Engenharia, Universidade do Algarve, Campus da Penha, 8005-139 Faro, Portugal. Tel.: +351 289 800100; fax: +351 289 888405.
E-mail address: cruivo@ualg.pt (C.R. Ruivo).

1290-0729/$ – see front matter © 2009 Elsevier Masson SAS. All rights reserved.
doi:10.1016/j.ijthermalsci.2009.04.004

Nomenclature

a_s	specific transfer area of the matrix, $m^2\,m^{-3}$
$c_{p,f}$	specific heat of the air flow, $J\,kg^{-1}\,K^{-1}$
$c_{p,p}$	specific heat of porous medium, $J\,kg^{-1}\,K^{-1}$
$\bar{c}_{p,p}$	average specific heat of the wall, $J\,kg^{-1}\,K^{-1}$
$c_{p,v}$	specific heat of water vapour, $J\,kg^{-1}\,K^{-1}$
D_f	diffusion coefficient of water vapour in the airflow, $m^2\,s^{-1}$
$D_{K,eff}$	effective coefficient of Knudsen diffusion, $m^2\,s^{-1}$
$D_{s,eff}$	effective coefficient of surface diffusion (of adsorbed water), $m^2\,s^{-1}$
d_{hyd}	hydraulic diameter, m
H_p	thickness of the desiccant layer, m
h_{ads}	heat of adsorption, $J\,kg^{-1}$
$h_{ads,p}$	average heat of adsorption, $J\,kg^{-1}$
h_h	convection heat transfer coefficient, $W\,m^{-2}\,K^{-1}$
h_{fg}	latent heat of vaporization, $J\,kg^{-1}$
h_l	enthalpy of liquid water, $J\,kg^{-1}$
h'_l	enthalpy of adsorbed water, $J\,kg^{-1}$
h_m	convection mass transfer coefficient, $m\,s^{-1}$
h_v	enthalpy of vapour, $J\,kg^{-1}$
h'_w	heat of wetting, $J\,kg^{-1}$
j_h	convective heat flux, $W\,m^{-2}$
j_m	convective mass flux, $kg\,s^{-1}\,m^{-2}$
Le	Lewis number
M_v	molecular mass of water, $kg\,kmol^{-1}$
Nu	Nusselt number
p	pressure of the air–vapour mixture, Pa
p_v	partial pressure of water vapour, Pa
$p_{v,sat}$	saturation pressure of water vapour, Pa
R_{gv}	particular gas constant of the air–vapour mixture, $J\,kg^{-1}\,K^{-1}$
R_v	particular gas constant of water vapour, $J\,kg^{-1}\,K^{-1}$
r_{gv}	average radius of pore volume occupied by the gaseous phase, m
S_{ads}	source-term in the energy conservation equation (2), $W\,m^{-3}$
Sh	Sherwood number
S_{v-l}	source-term in the mass conservation equation (1), $kg\,s^{-1}\,m^{-3}$
T	temperature, °C
T_i	temperature of the interface, °C
T_f	temperature of the airflow, °C
T_p	average temperature of the wall, °C
T_0	initial temperature in the porous medium, °C
t	time, s
U_h	overall heat transfer coefficient, $W\,m^{-2}\,K^{-1}$
U_m	overall mass transfer coefficient, $m\,s^{-1}$
w_v	water-vapour content of the gas mixture inside the porous medium (db), $kg\,kg^{-1}$
X_l	adsorbed water content (db), $kg\,kg^{-1}$
$X_{l,p}$	average adsorbed water content (db), $kg\,kg^{-1}$
$X_{l,0}$	initial adsorbed water content in the porous medium, $kg\,kg^{-1}$
y	spatial coordinate, m

Greek symbols

ε_{gv}	volume fraction of the gaseous mixture within the porous medium
ε_m	matrix porosity
φ_v	vapour mass fraction of the gas mixture inside the porous medium, $kg\,kg^{-1}$
$\varphi_{v,f}$	vapour mass fraction in the airflow, $kg\,kg^{-1}$
$\varphi_{v,i}$	vapour mass fraction of the gas mixture at the interface, $kg\,kg^{-1}$
$\varphi_{v,p}$	average vapour mass fraction of the gas mixture in the wall, $kg\,kg^{-1}$
λ_f	thermal conductivity of the airflow, $W\,m^{-1}\,K^{-1}$
λ_p	thermal conductivity of the porous medium, $W\,m^{-1}\,K^{-1}$
ρ^*_d	apparent density of the dry desiccant, $kg\,m^{-3}$
$\rho_{d,p}$	average apparent density of the dry desiccant, $kg\,m^{-3}$
ρ_f	density of the airflow, $kg\,m^{-3}$
ρ_{gv}	density of the fluid inside the porous medium, $kg\,m^{-3}$
ρ^*_{gv}	apparent density of the gas mixture inside the porous medium, $kg\,m^{-3}$
τ_l	tortuosity of the adsorbed water path within the porous medium
τ_{gv}	tortuosity of the water vapour path
ψ	relative pressure, i.e., ratio of the partial vapour pressure to the saturation vapour pressure

Superscripts

*	apparent density
′	adsorbed water

Subscripts

0	initial condition
ads	relative to the adsorption phenomenon
d	dry desiccant
eff	effective quantity
eq	equilibrium conditions
f	airflow
gv	gaseous mixture (air–vapour)
h	heat
i	solid–airflow interface
m	mass
p	porous medium
sat	saturation condition
v	water vapour
l	free liquid water or adsorbed water

simplified methods [21,24,25], as well as providing guidelines for the optimisation of the wheel performance [21,26].

In the present work, the numerical modelling of the behaviour of a layer of a desiccant composite is addressed, considering the complete set of governing equations for the local sorption, heat conduction and mass diffusion phenomena within the porous medium. The dependence of the thermodynamic properties, the diffusion coefficients and the volume fraction of the gaseous phase on the local primary variables (temperature, vapour and adsorbed water contents) is also considered. It is also supposed that the desiccant layer belongs to the channel wall of a compact exchanger, which is crossed by a moist air–vapour flow. The hypothesis of one-dimensionality assumed in this study – a plane and short element of the desiccant layer – is mainly intended to determine the overall transfer coefficients to be used in the pseudo-gas-side-controlled model.

2. Mathematical modelling

2.1. Detailed model

Although the channel geometry of a real hygroscopic matrix is three-dimensional, the modelled domain is reduced to an element

of the channel wall and considered one-dimensional. This assumption simplifies significantly the analysis of the heat and mass transfer phenomena inside the porous medium, towards the main purpose of investigating the overall transfer coefficients to be used in the PGSCM. Consequently, the physical domain of the problem is schematically represented in Fig. 1, in which only the channel wall element is studied. It is considered as a homogeneous desiccant medium with the properties of silica gel and having an infinitesimal-length in the flow direction. The half-thickness of the wall is related with the porosity and the specific area of the real hygroscopic matrix by $H_p = (1-\varepsilon_m)/a_s$.

Inside the porous medium, vapour and adsorbed water coexist in equilibrium, which is characterized by the water vapour–silica gel sorption isotherm. Due to the small dimension of the silica gel pores, only two mechanisms of mass transport are considered: surface diffusion of adsorbed water and Knudsen diffusion of water vapour [27]. The mass transport of dry-air inside the pores is also neglected and the total pressure is assumed to be constant and uniform.

At the interface between the airflow and the desiccant layer, transfer of water vapour and of heat occurs. The upper face of the desiccant layer is located at the symmetry plane relatively to an adjacent channel, and consequently is treated as an adiabatic and impermeable boundary.

The air stream in contact with the infinitesimal-length wall element is treated as a well mixed flow (bulk flow), characterized by constant and uniform properties (pressure, temperature and vapour content).

The governing equations can be mathematically deduced from appropriate balances applied to an infinitesimal control volume of the desiccant porous medium, leading to the following partial differential equations:

- mass conservation of adsorbed water:

$$\frac{\partial\left(\rho_d^* X_l\right)}{\partial t} = \frac{\partial}{\partial y}\left(D_{s,eff}\frac{\partial\left(\rho_d^* X_l\right)}{\partial y}\right) + S_{v-l} \tag{1}$$

- energy conservation in the porous medium (gas mixture, adsorbed water and desiccant solid):

$$\frac{\partial}{\partial t}\left(\rho_d^* \cdot c_{p,p} \cdot T\right) = \frac{\partial}{\partial y}\left(\lambda_p \frac{\partial T}{\partial y}\right) + S_{ads}. \tag{2}$$

The local value of the vapour mass fraction ϕ_v is specified as the equilibrium value, obtained from the sorption isotherm as a function of the local values of T and X_l [28]. The source-term S_{v-l} represents the adsorption rate per unit volume of the porous medium and is expressed by

$$S_{v-l} = \frac{\partial}{\partial y}\left(\frac{D_{K,eff}}{\varepsilon_{gv}} \cdot \frac{\partial\left(\rho_{gv}^* \varphi_v\right)}{\partial y}\right) - \frac{\partial\left(\rho_{gv}^* \varphi_v\right)}{\partial t}. \tag{3}$$

The energy equation (2) is written in a classical form, in terms of temperature as the primary dependent variable. From the mathematical derivation of that equation, the following expression results:

$$S_{ads} = \rho_d^* \frac{\partial\left(X_l h'_w\right)}{\partial t} + \frac{\partial}{\partial y}\left(D_{s,eff}\frac{\partial\left(\rho_d^* X_l\right)}{\partial y} h'_w\right) + \frac{\partial}{\partial y}\left(\frac{D_{K,eff}}{\varepsilon_{gv}} \cdot \frac{\partial\left(\rho_{gv}^* \varphi_v\right)}{\partial y} h_v\right) - \frac{\partial\left(\varphi_v \rho_{gv}^* h_{fg}\right)}{\partial t}. \tag{4}$$

The specific enthalpy of the water vapour is given by

$$h_v = c_{p,v} T + h_{fg} \tag{5}$$

and that of the adsorbed water is given by

$$h'_l = h_v - h_{ads} \tag{6a}$$

or, by other means:

$$h'_l = h_l - h'_w, \tag{6b}$$

where h_{ads} is the heat of adsorption and h'_w is the heat of wetting.

The instantaneous volume fraction ε_{gv} is the ratio between the instantaneous volume occupied by the air–vapour mixture in the pores and the total volume of the solid porous medium, being correlated with the local content of adsorbed water.

The effective diffusivity associated with Knudsen diffusion in a porous desiccant medium may be written as [28]:

$$D_{K,eff} = 97 r_{gv}\sqrt{\frac{T+273.15}{R_v}}\frac{\varepsilon_{gv}}{\tau_{gv}}. \tag{7}$$

The effective diffusivity associated to the surface diffusion of adsorbed water $D_{s,eff}$ in a porous desiccant medium is directly influenced by the path tortuosity, τ_l, and depends on the pair adsorbate–adsorbent. In the present work, the following expression was used [28]:

$$D_{s,eff} = \frac{D_{s0}}{\tau_l} \cdot \exp\left(\frac{-4.5\times10^{-4} h_{ads}}{b R_v (T+273.15)}\right), \tag{8}$$

where b depends on the type of adsorption bond and D_{s0} is a constant that depends on the adsorbent.

The effective thermal conductivity of the porous medium λ_p is difficult to predict accurately due to the coupled transfer phenomena. An average value is used according to the conductivity and mass fraction of each component phase. A similar procedure is used to evaluate the specific heat of the porous medium.

The moisture content of the air–vapour mixture w_v (mass fraction of vapour on dry basis) is calculated from the vapour mass fraction ϕ_v through

$$w_v = \frac{\varphi_v}{(1-\varphi_v)}. \tag{9}$$

The upper and the two lateral faces of the wall element are considered adiabatic, as well as impermeable to both water phases

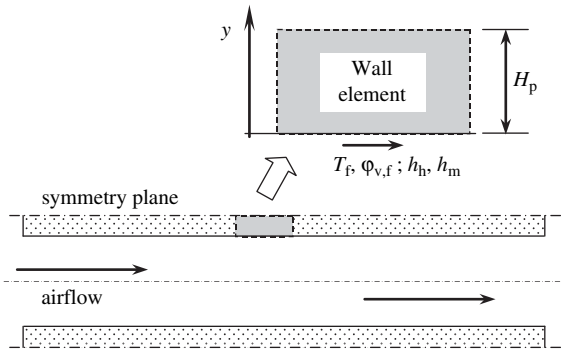

Fig. 1. Schematic representation of the airflow channel and of the calculation domain – a wall element.

(cf. Fig. 1). According to the low-mass-transfer rate theory [29], the mass and heat fluxes evaluated on the gas side of the interface are

$$j_m = h_m \cdot \rho_f \left(\varphi_{v,f} - \varphi_{v,i}\right) \tag{10}$$

and

$$j_h = h_h \left(T_f - T_i\right), \tag{11}$$

respectively, where $\varphi_{v,i}$ and T_i are instantaneous values at the interface and $\varphi_{v,f}$ and T_f are instantaneous bulk flow values. The convection heat and mass transfer coefficients are taken from the values of the Nusselt and the Sherwood numbers for the fully-developed laminar regime of an internal channel flow, which are related by the well-known Chilton–Colburn analogy:

$$Sh = Nu \cdot Le^{1/3}, \tag{12}$$

the Lewis number being estimated from its definition:

$$Le = \frac{\lambda_f}{\left(\rho_f c_{p,f} D_f\right)}. \tag{13}$$

The convection coefficients are then obtained by the expressions:

$$h_h = Nu \cdot \lambda_f / d_{hyd} \tag{14}$$

and

$$h_m = Sh \cdot D_f / d_{hyd}. \tag{15}$$

The interface fluxes calculated through equations (10) and (11) are positive in the y direction, i.e., when entering the wall element (cf. Fig. 1).

At the interface with the airflow, the following surface balances can be written:

$$\left[-\frac{D_{K,eff}}{\varepsilon_{gv}} \cdot \frac{\partial\left(\rho^*_{gv}\varphi_v\right)}{\partial y} - D_{s,eff} \frac{\partial\left(\rho^*_d X_l\right)}{\partial y} \right]_{y=0^+} = h_m \cdot \rho_f \left(\varphi_{v,f} - \varphi_{v,i}\right) \tag{16}$$

and

$$\left[-\frac{D_{K,eff}}{\varepsilon_{gv}} \cdot \frac{\partial\left(\rho^*_{gv}\varphi_v\right)}{\partial y} h_v - D_{s,eff} \frac{\partial\left(\rho^*_d X_l\right)}{\partial y} h'_l - \lambda_p \frac{\partial T}{\partial y} \right]_{y=0^+} = h_h \left(T_f - T_i\right) + h_m \cdot \rho_f \left(\varphi_{v,f} - \varphi_{v,i}\right) \cdot h_{v,i}. \tag{17}$$

The partial differential equations (1) and (2) are discretized using the finite volume method [30] and solved through the tri-diagonal matrix algorithm (TDMA). An iterative procedure is performed in each time step, in order to handle the strong coupling between the governing equations and the non-linearities implied by the changing properties. With appropriate control parameters, the resulting numerical model showed a rather stable and robust behaviour along the calculation procedure.

The calculation domain is divided into control-volumes, forming a cartesian and non-uniform grid, which is gradually expanded from the solid–flow interface towards the adiabatic/impermeable upper surface. A very short distance from the first inner grid point to the interface is imposed (0.5–1 μm), thus ensuring an accurate numerical representation of the boundary conditions expressed by equations (16) and (17). These boundary conditions are introduced via the corresponding source-terms in the discretization equations [30]. Since the present study is focused on the evaluation of the overall transfer coefficients of the PGSCM, the numerical model is assumed one-dimensional and solved only for one column of control-volumes.

The time discretization consists of a step-by-step evolution, each time interval being automatically generated along the numerical simulation of the transient process. Basically, the sharper is the time evolution of the dependent variables the shorter are the time steps imposed, and conversely. This generation algorithm guarantees a suitable representation of the transient evolutions, while minimizing the computing time needed to simulate a complete adsorption or desorption process.

Further information and results of the detailed numerical modelling of the channel wall element can be found in [21,24–26].

2.2. Pseudo-gas-side-controlled model – PGSCM

The simulation of the behaviour of the channel wall element with the PGSCM is achieved solving the two following equations for the mass and energy conservation:

$$\frac{\partial\left(\rho^*_{d,p} X_{l,p}\right)}{\partial t} = \frac{1}{H_p} U_m \rho_f \left(\varphi_{v,f} - \varphi_{v,p}\right) \tag{18}$$

and

$$\frac{\partial\left(\rho^*_{d,p} \bar{c}_{p,p} T_p\right)}{\partial t} = \frac{U_m \rho_f \left(\varphi_{v,f} - \varphi_{v,p}\right) h_{ads,p} + U_h \left(T_f - T_p\right)}{H_p}. \tag{19}$$

In this simplified formulation, it is assumed that there are no gradients inside the desiccant layer of the wall element, and that the average values of $X_{l,p}$, T_p and $\varphi_{v,p}$ represent also the state of the solid–gas interface. These three variables are related by the sorption isotherm under the hypothesis of local hydrothermal equilibrium [28]. The variables U_m and U_h are pseudo-overall transfer coefficients that must be known. The pseudo-simplified model PGSCM corresponds exactly to the gas-side-controlled model (GSCM) when with $U_m \approx h_m$ and $U_h \approx h_h$.

3. Results and discussion

The detailed model presented above is a powerful tool to investigate the values of the overall coefficients to use in the PGSCM. Taking the value of the convective heat flux predicted by the detailed model, equation (11), the overall heat coefficient is calculated by

$$U_h = \frac{j_h}{T_f - T_p}, \tag{20}$$

where T_p is the mean value of the temperature calculated after the solution of the detailed model is given by

$$T_p = \frac{1}{H_p} \int_{y=0}^{y=H_p} \frac{\rho^*_{d,p} \bar{c}_{p,p} T}{\rho^*_{d,p} \bar{c}_{p,p}} \, dy. \tag{21}$$

In a similar way, the overall mass coefficient is calculated after the convective mass flux predicted by the detailed model, equation (10), as follows:

$$U_m = \frac{j_m}{\rho_f \left(\varphi_{v,f} - \varphi_{v,p}\right)}, \tag{22}$$

Table 1
Airflow and initial conditions of the desiccant wall for both the adsorption and desorption processes simulated.

	Adsorption	Desorption
T_f (°C)	30	100
$w_{v,f}$ (kg kg^{-1})	0.01	0.01
p (Pa)	101,325	101,325
T_0 (°C)	100	30
$X_{l,0}$ (kg kg^{-1})	0.0126	0.2363

where $\varphi_{v,p}$ is determined by the sorption isotherm [28] as a function of T_p and $X_{l,p}$, this one given by

$$X_{l,p} = \frac{1}{H_p}\int_{y=0}^{y=H_p} X_l \, dy. \quad (23)$$

The variables T_f, ρ_f and $\varphi_{v,f}$ refer to the state of the bulk airflow, which, in the present simulation of the channel element, correspond exactly to the specified airflow conditions.

Starting from a given initial state, the response of the desiccant wall to a step change of the airflow conditions was simulated until final equilibrium was achieved. Table 1 summarizes the input data for the calculations, namely the imposed state of the airflow and the initial conditions of the desiccant wall.

The value 2.45 was assigned to the Nusselt number corresponding to heat convection between a uniform temperature wall and a fully-developed laminar flow inside a corrugate sinusoidal-type channel of a compact exchanger [9]. The channel cross-section area was 4.5 mm^2, with an internal perimeter of 10.6 mm and a hydraulic diameter of 1.69 mm, approximately.

Runs were conducted with the detailed modelling covering a wide range of values of the layer thickness (0.01–5 mm).

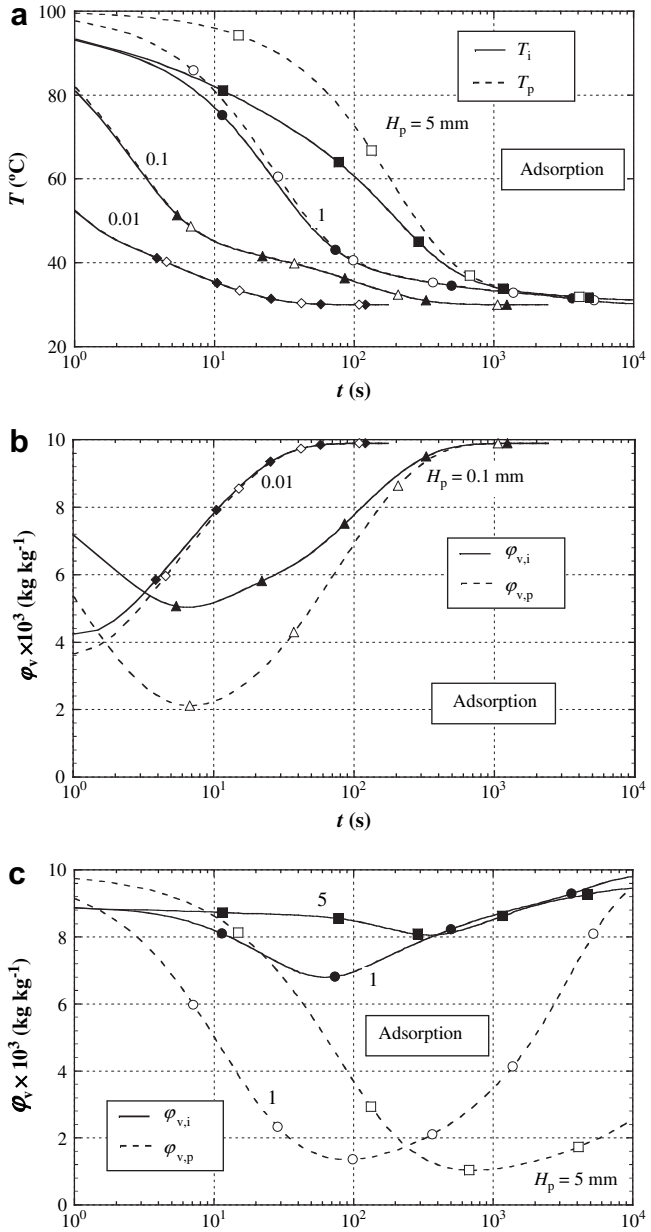

Fig. 2. Time evolutions during the adsorption process: (a) temperatures T_p and T_i; (b) and (c) vapour mass fractions $\varphi_{v,p}$ and $\varphi_{v,i}$.

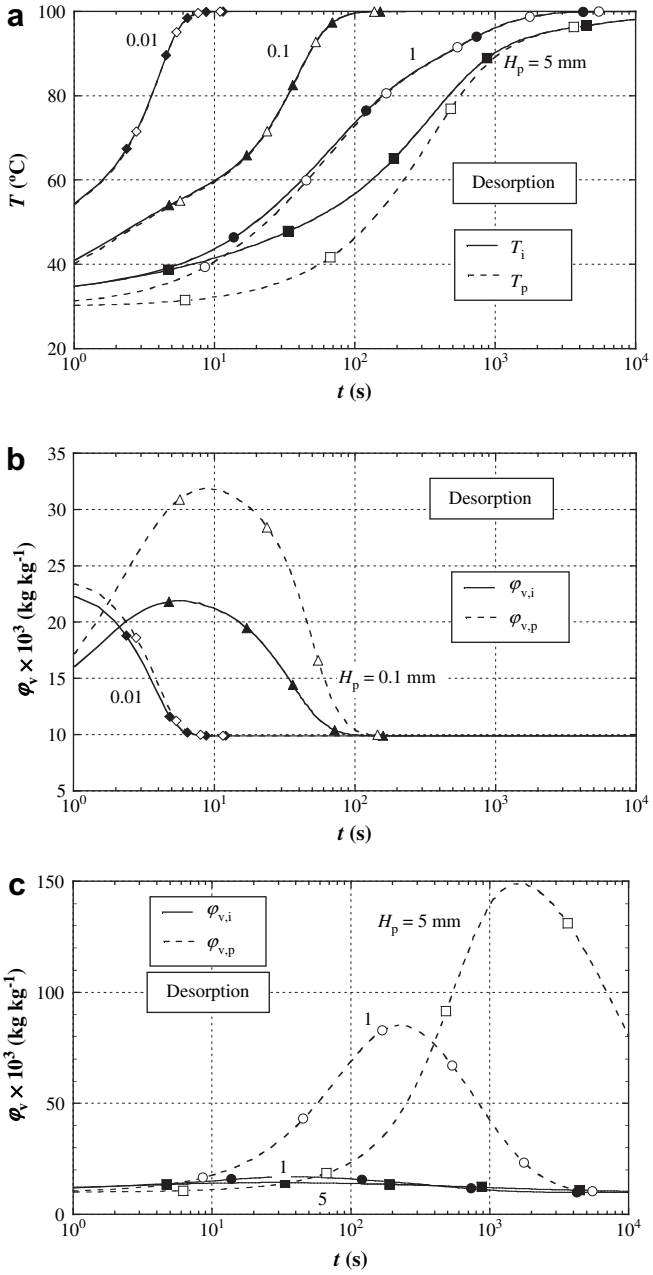

Fig. 3. Time evolutions during the desorption process: (a) temperatures T_p and T_i; (b) and (c) vapour mass fractions $\varphi_{v,p}$ and $\varphi_{v,i}$.

The fluid properties of the binary air–vapour mixture depend on the primary variables T and φ_v. Appropriate φ_v-weighted functions were developed that take into account the individual dry-air and water-vapour properties available from thermodynamic tables [31]. The properties of the desiccant medium are referred to silica gel RD [28].

Fig. 2 shows the calculated evolutions of the mean state of the wall (T_p and $\varphi_{v,p}$) and of the state of the interface (T_i and $\varphi_{v,i}$) for the cases of adsorption in desiccant layers of different thickness in the range of 0.01–5 mm. Fig. 3 shows the corresponding evolutions for the desorption cases.

Figs. 4 and 5 represent the evolutions of the overall transfer coefficients U_h and U_m for the adsorption and desorption processes, respectively, calculated with equations (20) and (22).

Coefficients U_h and U_m in Figs. 4 and 5, for $H_P = 0.01$ mm, are approximately constant and agree well with the respective values of the convective coefficients h_h and h_m, derived form the Nusselt and Sherwood numbers. However, the values of U_h and U_m differ much from the adsorption to the desorption process, due to the influence of the airflow properties on the convective coefficients (cf. equations (14) and (15)).

For $H_P = 0.1$ mm, a reasonable agreement between the evolution of U_h and h_h is also observed, while U_m exhibits a weak variation during the adsorption process and shows a non-negligible decrease during the desorption process. For $H_P = 1$ mm, a deviation of U_h relatively to the imposed value of h_h is observed, as well as variations during the process. For $H_P = 5$ mm, the deviations and the transient variations are much more remarkable.

For $H_P = 1$ mm and for $H_P = 5$ mm, the evolutions of the coefficient U_m evidence a strong decreasing during the process, with the particularity that the values of U_m at the beginning are higher than the imposed values of h_m. So, this could mean that the

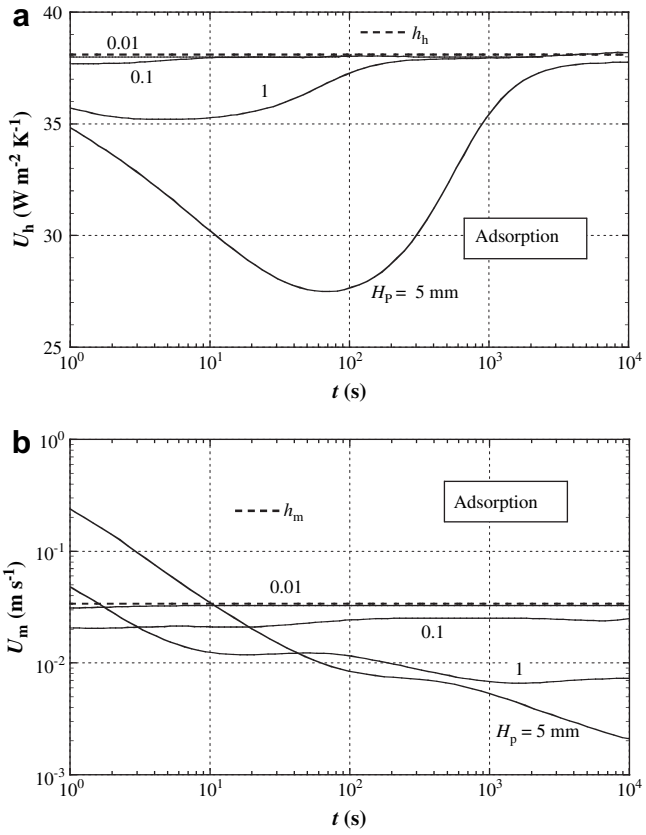

Fig. 4. Transient evolutions of the overall coefficients for (a) heat transfer U_h, and (b) mass transfer U_m, during the adsorption process.

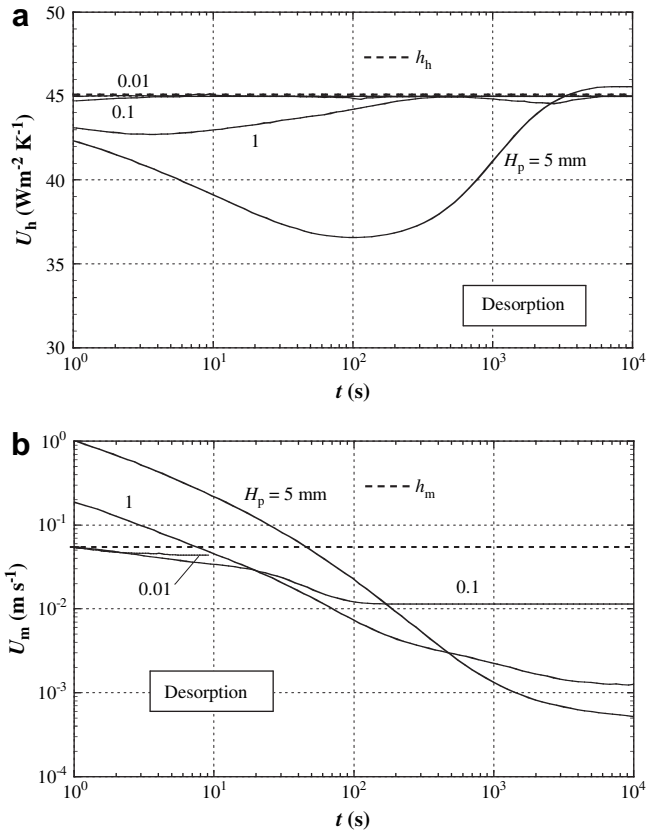

Fig. 5. Transient evolutions of the overall coefficients for (a) heat transfer U_h, and (b) mass transfer U_m, during the desorption process.

global resistance to the mass transfer, during at the beginning of this transient process, is smaller than the convective resistance, which contraries the physics law of the transfer phenomena. An accurate analysis of the evolution of $\varphi_{v,i}$ and $\varphi_{v,p}$ can help to understand this apparent absurd. In fact, at the beginning the potential for convection mass transfer $(\varphi_{v,f} - \varphi_{v,i})$ is greater than the potential $(\varphi_{v,p} - \varphi_{v,p})$ adopted in the simplified modelling (v., Fig. 2c). So, to assure the same convective mass flux when predicted by the model PGSCM, a U_m value artificially augmented must be adopted. This fact also helps to justify the classification of "Pseudo" for this simplified model.

From the present analysis, it can be concluded that the use of the model PGSCM is easy and reliable for $H_p < 0.1$ mm. On the other hand, it can be used for $H_p > 0.1$ mm only if an empiric law, enabling the estimation of the variations of the coefficients U_h and U_m, exists. Some investigations focusing this last point were performed, concluding that it is not an easy task to find a generic law for that purpose, particularly for U_m.

4. Conclusions

A detailed mathematical model was formulated in order to describe the behaviour of a wall element of a desiccant matrix. A one-dimensional version of it was used under specific conditions, aiming to estimate the overall heat and mass transfer coefficients that are required to use as input data in pseudo-gas-side-controlled models.

The capabilities of the detailed model were demonstrated, namely through the predicted transient evolutions of the primary variables (temperature, vapour and adsorbed water contents), as well as the transient heat and mass fluxes at the interface.

It was also concluded that, for both the adsorption and desorption processes simulated, the heat and mass lumped capacitance assumption supporting the gas-side-controlled model is valid only for desiccant layers thinner than about 0.1 mm, in which cases $U_m \approx h_m$ and $U_h \approx h_h$. The main conclusion of the present work is that, for thicker desiccant layers, difficulties still subsist in the use of simplified models PGSCM, due to the significant variations of U_h and U_m during the transient process, which are extremely difficult to predict accurately.

References

[1] I.L. Maclaine-Cross, P.J. Banks, Coupled heat and mass transfer in regenerators-prediction using an analogy with heat transfer, Int. J. Heat Mass Transfer 15 (6) (1972) 1225–1242.
[2] P.J. Banks, Coupled equilibrium heat and single adsorbate transfer in fluid flow through a porous medium – I. Characteristic potentials and specific capacity ratios, Chem. Eng. Sci. 27 (5) (1972) 1143–1155.
[3] E. Van Den Bulk, J.W. Mitchell, S.A. Klein, Design theory for rotary heat and mass exchangers – I. Wave analysis of rotary heat and mass exchangers with infinite transfer coefficients, Int. J. Heat Mass Transfer 28 (8) (1985) 1575–1586.
[4] E. Van Den Bulk, J.W. Mitchell, S.A. Klein, Design theory for rotary heat and mass exchangers – II. Effectiveness–number-of-transfer-units method for rotary heat and mass exchangers, Int. J. Heat Mass Transfer 28 (8) (1985) 1587–1595.
[5] W. Zheng, W.M. Worek, Numerical simulation of combined heat and mass transfer processes in a rotary dehumidifier, Numer. Heat Transfer A – Appl. 23 (2) (1993) 211–232.
[6] J.Y. San, S.C. Hsiau, Effect of axial solid heat conduction and mass diffusion in a rotary heat and mass regenerator, Int. J. Heat Mass Transfer 36 (8) (1993) 2051–2059.

[7] C.C. Ni, J.Y. San, Mass diffusion in a spherical microporous particle with thermal effect and gas-side mass transfer resistance, Int. J. Heat Mass Transfer 43 (12) (2000) 2129–2139.
[8] Y.J. Dai, R.Z. Wang, H.F. Zhang, Parameter analysis to improve rotary desiccant dehumidification using a mathematical model, Int. J. Therm. Sci. 40 (4) (2001) 400–408.
[9] X.J. Zhang, Y.J. Dai, R.Z. Wang, A simulation study of heat and mass transfer in a honeycomb rotary desiccant dehumidifier, Appl. Therm. Eng. 23 (8) (2003) 989–1003.
[10] M.N. Golubovic, W.M. Worek, Influence of elevated pressure on sorption in desiccant wheels, Numer. Heat Transfer A – Appl. 45 (9) (2004) 869–886.
[11] Z. Gao, V.C. Mei, J.J. Tomlinson, Theoretical analysis of dehumidification process in a desiccant wheel, Heat Mass Transfer 41 (11) (2005) 1033–1042.
[12] T.S. Ge, Y. Li, R.Z. Wang, Y.J. Dai, A review of the mathematical models for predicting rotary desiccant wheel, Renew. Sust. Energy Rev. 12 (6) (2008) 1485–1528.
[13] E. Van den Bulk, S.A. Klein, A single-blow test procedure for compact heat and mass exchangers, J. Heat Transfer-ASME 112 (2) (1990) 317–322.
[14] A.A. Pesaran, A. Mills, Moisture transport in silica gel packed beds – II. Experimental study, Int. J. Heat Mass Transfer 30 (6) (1987) 1051–1060.
[15] M. Beccali, F. Butera, R. Guanella, R.S. Adhikari, Simplified models for the performance evaluation of desiccant wheel dehumidification, Int. J. Energy Res. 27 (1) (2003) 17–29.
[16] H.I. Henderson, J.R. Sand, An hourly building simulation tool to evaluate hybrid desiccant system configuration options, ASHRAE Trans. 109 (2) (2003) 551–564.
[17] L.A. Sphaier, W.M. Worek, Analysis of heat and mass transfer in porous sorbents used in rotary regenerators, Int. J. Heat Mass Transfer 47 (14–16) (2004) 3415–3430.
[18] P. Majumdar, Heat and mass transfer in composite pore structures for dehumidification, Sol. Energy 62 (1) (1998) 1–10.
[19] J.L. Niu, L.Z. Zhang, Effects of wall thickness on the heat and moisture transfer in desiccant wheels for air dehumidification and enthalpy recovery, Int. Commun. Heat Mass Transfer 29 (2) (2002) 255–268.
[20] L.Z. Zhang, J.L. Niu, A pre-cooling Munters environmental control desiccant cooling cycle in combination with chilled-ceiling panels, Energy 28 (3) (2003) 275–292.
[21] C.R. Ruivo, Modelação numérica dos fenómenos de transferência de calor e de massa em rodas higroscópicas, Ph.D. thesis, University of Coimbra, Coimbra, Portugal, 2005 (in Portuguese).
[22] C.R. Ruivo, J.J. Costa, A.R. Figueiredo, On the behaviour of hygroscopic wheels: part I – channel modelling, Int. J. Heat Mass Transfer 50 (23–24) (2007) 4812–4822.
[23] C.R. Ruivo, J.J. Costa, A.R. Figueiredo, On the behaviour of hygroscopic wheels: part I – channel modelling, Int. J. Heat Mass Transfer 50 (23–24) (2007) 4823–4832.
[24] C.R. Ruivo, J.J. Costa, A.R. Figueiredo, Analysis of simplifying assumptions for the numerical modeling of the heat and mass transfer in a porous desiccant medium, Numer. Heat Transfer A 49 (9) (2006) 851–872.
[25] C.R. Ruivo, J.J. Costa, A.R. Figueiredo, On the validity of lumped capacitance approaches for the numerical prediction of heat and mass transfer in desiccant airflow systems, Int. J. Therm. Sci. 47 (3) (2008) 282–292.
[26] C.R. Ruivo, J.J. Costa, A.R. Figueiredo, Numerical study of the behavior of an elementary desiccant layer of a hygroscopic rotor, Numer. Heat Transfer A 53 (10) (2008) 1037–1053.
[27] A.A. Pesaran, A. Mills, Moisture transport in silica gel packed beds – I. Theoretical study, Int. J. Heat Mass Transfer 30 (6) (1987) 1037–1049.
[28] A. Pesaran, Moisture transport in silica gel particle beds, Ph.D. thesis, University of California, Los Angels, USA, 1983.
[29] A.F. Mills, Heat and Mass Transfer, Irwin, 1995.
[30] S.V. Patankar, Numerical Heat Transfer and Fluid Flow, Hemisphere, McGraw-Hill, Washington, DC, 1980.
[31] Y. Çengel, Heat Transfer – A Practical Approach, McGraw-Hill, New York, 1998.